Proceedings of the 3rd World Congress on Mechanical, Chemical, and Material Engineering (MCM'17)
Rome, Italy – June 8 – 10, 2017
Paper No. HTFF 152
ISSN: 2369-8136
DOI: 10.11159/htff17.152

Effect of Surface Roughness on Non-Equilibrium Condensation in a Laval Nozzle

Aditya Pillai, B. V. S. S. S. Prasad
Turbo Machines Lab, Indian Institute of Technology Madras
Chennai 600036, India
adityapillai009@gmail.com; prasad@iitm.ac.in

Abstract **-** The present study focuses on the effects of different surface roughness of the walls of a Laval nozzle on the non-equilibrium condensation of steam. The study describes the result of a numerical investigation of wet steam flow in a low-pressure convergent-divergent nozzle using commercial computational fluid dynamics package ANSYS Fluent 16. A 2D computational domain is considered and is discretized in a structured mesh with finer grid near the nozzle walls to capture the effects of roughness in the supersonic flow of steam. The mathematical model describing the phase change, which involves the formation of liquid droplets in a homogeneous non-equilibrium condensation process, is based on the classical nucleation theory. The Eulerian-Eulerian approach for modeling the wet steam has been adopted. The SST k-ω model has been used for the accurate formulation of the flow physics in the near wall region. The computational results for the case with no surface roughness were validated with the experimental results available in the literature provided by Moses and Stein were found to be in very good agreement. The pressure distribution, nucleation rate, average droplet radius and mass flow rate were compared for different values of surface roughness of nozzle walls. It is found out from the simulations that the parameters studied have a dependence on the surface roughness of the nozzle walls. There is a shift in the point of the incipience of the droplets and also in the nucleation rate. A reduction in the average droplet radius and the nucleation rate with increase in surface roughness along with a reduction in the condensation shock strength of rough nozzles when compared with the nozzle with no surface roughness is observed.

Keywords**:** surface roughness, condensation, wet steam, nozzle, non-equilibrium, two-phase flow

1. Introduction

Two-phase condensing flows are very common in many technical applications, such as rotating machinery operating with steam and nuclear reactors. The occurrence of condensation can lead to a degradation of a component's performance. Thermodynamic irreversible losses, generated with non-equilibrium conditions and phase change, are significant to the low-pressure stage efficiency since for every additional percent of wetness the efficiency is reduced by approximately 1% [1]. Thus, the physical understanding of the condensation process can be of great help in the design process.

Steam turbines are widely used in the power industry for the efficient generation of power. The largest portion of the power produced by a steam turbine is generated from the low-pressure stages. As the flow expands and the state path crosses the vapour saturation curve, steam first supercools and then nucleates to become a two-phase mixture. The water droplets grow and release their latent heat to the flow and this heat addition to the flow causes a rise in the pressure which is called condensation shock. Different studies have been performed to better understand the non-equilibrium condensation process and how it affects the performance of a turbine [2-5]. The modeling of condensation process of wet steam has been extensively investigated for several years by Wegener et al. [6] and Gyarmathy [7,8]. Since the devices in which the condensation process takes place are extremely complex, it makes it quite difficult to model and conduct numerical and experimental research. On the other hand, a simple model for simulating complex flows in practical domains is a converging-diverging nozzle.

During the operation of steam turbines, the blade surfaces experience severe performance degradation. Erosion of blades due to heat, the collision of particles or impurities and deposition of impurities on the blade's surface significantly affect the surface roughness of the blades. The problems related to the blade surface roughness are well known among the people working on turbomachinery design. A large quantity of experimental and numerical work has been done on the performance losses of turbines due to blade surface roughness [9-13]. Despite the abundance of data available for the

condensation in a Laval nozzle by Moses and Stein, Dykas et al. and Bakhtar et al. [14-16], no attempts have been made to study the effect of different surface roughness values on the non-equilibrium condensation process. The present communication makes an effort in that direction.

Nomenclature

C_s = Roughness constant
D_ω = Cross diffusion term
G_k, G_ω = Generation of k and ω
h_q = Specific enthalpy of q^{th} phase
h_{pq} = Interphase enthalpy
I = Nucleation rate
K_s = Equivalent sand grain roughness height
k = Turbulent kinetic energy
m_{in} = Mass flow rate at inlet
m_{out} = Mass flow rate at outlet
p = static pressure
p_o = Total inlet pressure
Q_{pq} = Intensity of heat exchange between p^{th} and q^{th} phase
$\vec{q}_q$ = Heat flux
S_k, S_ω = User defined source terms
S_q = Source term
$\vec{v}$ = Velocity vector
X = Axial distance
Y_k, Y_ω = Dissipation of k and ω
y+ = Non-dimensional wall distance

Greek Letters

ρ = Density
β= Wetness factor
η = Number density of droplets per unit volume
ω = Specific dissipation rate
Γ = Mass generation rate due to condensation
Γ_k, Γ_ω = Effective diffusivity of k and ω

2. Geometry & Computational Domain

The computational domain consists of a two-dimensional converging-diverging Laval nozzle geometry for which the experimental data is made available by Moses and Stein [15]. The actual geometry of the nozzle, as shown in Fig. 1, was chosen by the respective authors for the ease of fabrication with the additional criterion of curve continuity through the second derivative in the transonic and supersonic positions. A circular arc was chosen for the profile of a subsonic and transonic section of the nozzle with 0.053 m and 0.686 m radius respectively meeting each other tangentially. The expansion rate defined as $\dot{P} = \frac{-1}{p}\frac{dp}{dt}$, of the nozzle was found out to be 8,230 sec-1.

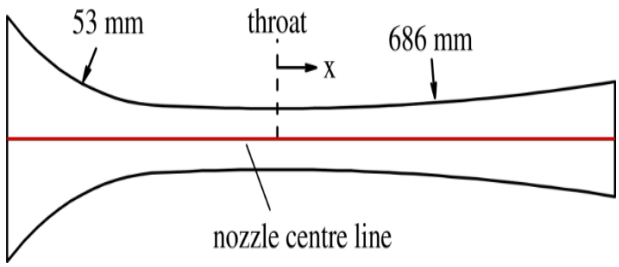

Fig. 1: Actual nozzle geometry.

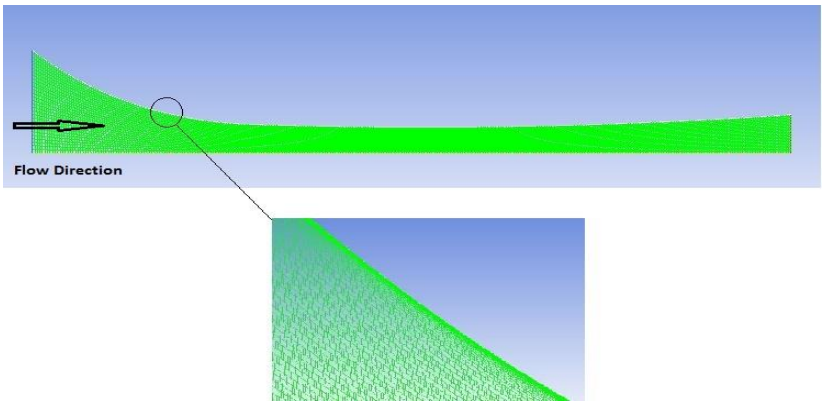

Fig. 2: Computational domain and the mesh.

Fig. 2 shows the mesh adopted for the simulation of the wet steam flow through the nozzle. Grid independence was achieved at 121,634 quadrilateral cells. A finer mesh at the nozzle walls ensured that the surface characteristics are properly captured and the desired y+ value is achieved. As the mesh is finer near the walls, the aspect ratio is very high. The convergence and accuracy may be impaired with a single-precision solver, due to inefficient transfer of boundary information and hence the double-precision version of the Ansys Fluent 16 is used. A convergence of 10^{-5} was obtained with the help of these settings.

3. Governing Equations & Boundary Conditions

The nozzle geometry is symmetric about the center line as the flow domain is axisymmetric. So, the symmetric condition is applied to the lower boundary of the geometry. The left and the right boundaries are specified as pressure-inlet and pressure-outlet boundary conditions, whereas the circular arcs are taken to be the nozzle walls.

The inlet total pressure of 70 kPa and temperature of 377 K (11 degrees supercooling) corresponds to the experiment 410 conducted by Moses and Stein. Different equivalent sand grain roughness heights K_s are specified for these boundary conditions at the wall assuming that the heights are uniform throughout, which defines the roughness constant $C_s = 0.5$.

As shown in Fig.3, the equivalent sand roughness depends on the arrangement (pattern), distance (density) and shape, of the roughness elements such as grooved, sand grains, waves or cuboids, therefore it is possible that these elements differentiate in roughness although they have the identical geometrical roughness height K. Plate-shaped roughness elements, for example, are about the same height as sand grains, but its roughness can be eight times bigger, depending on the distance between the plates (density). Nikuradse made very extensive and systematic measurements in rough pipes. The sand roughness, which was examined by Nikuradse can be characterized by a maximum roughness density. In many technical applications, the roughness density is substantially smaller. Such a roughness can no longer be indicated by a roughness height K. For this purpose, it has proved to classify the roughness by comparing it to a scale of a normal roughness and then choose the Nikuradse sand roughness. Four different equivalent sand grain roughness heights (K_s) of 1μm, 10μm, 100μm and 1mm spanning from smooth to fully rough regimes [9] were assigned to the wall of the nozzle and the influence of varying K_s on the pressure distribution, nucleation rate, average droplet radius and mass flow rate is studied.

The simulation in the present case is steady, one-dimensional, turbulent flow with attached supersonic expansion. The SST k-ω model is solved for turbulence. Wet steam model with classical nucleation theory is applied.

For effectively modeling the surface roughness effects in a turbulent wall bounded flow, the law-of-the-wall modified for roughness is used. Experiments in roughened pipes and channels indicate that the mean velocity distribution near rough walls, when plotted in the usual semi-logarithmic scale, has the same slope ($1/\kappa$) but a different intercept (additive constant B in the log-law). Therefore, the law-of-the-wall for mean velocity modified for roughness has the form

$$\frac{u_p u^*}{\tau_w/\rho} = \frac{1}{\kappa} ln\left(E\frac{\rho u^* y_p}{\mu}\right) - \Delta B \tag{1}$$

where, $u^* = C_\mu{}^{1/4} k^{1/2}$

$$\Delta B = \frac{1}{\kappa} ln f_r \tag{2}$$

where fr is a roughness function that quantifies the shift of the intercept due to roughness effects. For a sand-grain roughness and similar types of uniform roughness elements, however, ΔB has been found to be well-correlated with the nondimensional roughness height, Ks+= ρKsu*/μ, where Ks is the physical roughness height and $u^* = C_\mu{}^{1/4} k^{1/2}$. Formulas proposed by Cebeci and Bradshaw based on Nikuradse's data [18] are adopted to compute ΔB for each regime.

Hydrodynamically smooth regime (Ks+ <2.25) :

$$\Delta B = 0 \tag{3}$$

Transitional regime (2.25<K_s^+<90) :

$$\Delta B = \frac{1}{\kappa} ln\left[\frac{K_s{}^+ - 2.25}{87.75} + C_s K_s{}^+\right] \times \sin\{0.4258(\ln K_s{}^+ - 0.811)\} \tag{4}$$

Fully rough regime (K_s^+>90) :

$$\Delta B = \frac{1}{\kappa} ln(1 + C_s K_s{}^+) \tag{5}$$

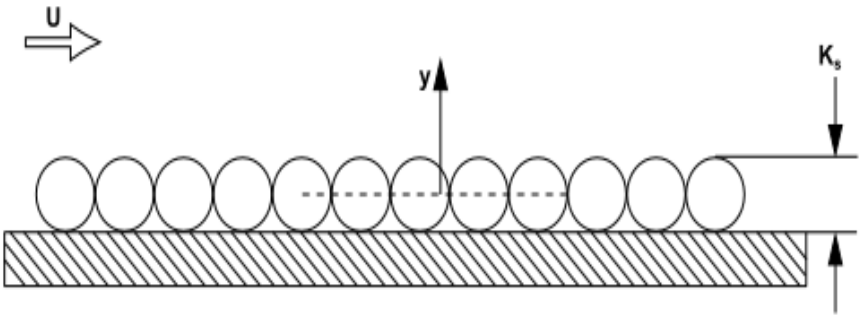

Fig. 3: Equivalent sand grain roughness K_s.

From the values of K_s and C_s, ΔB is calculated which is then used to evaluate the shear stress at the wall from (1) and also the other wall functions for the mean temperature and turbulent quantities.

The governing equations solved are as given below –

Conservation of mass:

$$\frac{\partial}{\partial x_j}(\rho u_j) = 0 \tag{6}$$

Conservation of momentum:

$$\frac{\partial}{\partial t}(\rho\vec{v}) + \nabla.(\rho\vec{v}\vec{v}) = -\nabla p + \nabla.(\bar{\bar{\tau}}) + \rho\vec{g} + \vec{F} \tag{7}$$

Conservation of energy:

$$\frac{\partial}{\partial t}(\alpha_q\rho_q h_q) + \nabla.(\alpha_q\rho_q\vec{u}_q h_q) = \alpha_q\frac{\partial p}{\partial t} + \bar{\bar{\tau}}_q:\nabla\vec{u}_q - \nabla\vec{q}_q + S_q + \sum_{p=1}^{n}(Q_{pq} + \dot{m}_{pq}h_{pq} - \dot{m}_{qp}h_{qp}) \tag{8}$$

Turbulence SST k-ω equation:

$$\frac{\partial}{\partial t}(\rho k) + \frac{\partial}{\partial x_i}(\rho k u_i) = \frac{\partial}{\partial x_j}\left(\Gamma_k\frac{\partial k}{\partial x_j}\right) + G_k - Y_k + S_k \tag{9}$$

$$\frac{\partial}{\partial t}(\rho\omega) + \frac{\partial}{\partial x_j}(\rho\omega u_j) = \frac{\partial}{\partial x_j}\left(\Gamma_\omega\frac{\partial \omega}{\partial x_j}\right) + G_\omega + S_\omega + D_\omega - Y_\omega \tag{10}$$

Wet Steam transport equations:

$$\frac{\partial}{\partial t}(\rho\beta) + \nabla.(\rho\vec{v}\beta) = \Gamma \tag{11}$$

$$\frac{\partial}{\partial t}(\rho\eta) + \nabla.(\rho\vec{v}\eta) = \rho I \tag{12}$$

4. Results and Discussions

Fig. 4 shows the pressure distribution along the center line of a converging-diverging nozzle with smooth walls. The black line represents the results obtained through numerical simulation and the red line shows the experimental data provided by Moses and Stein case 410. A reasonably good agreement was found between the numerical and experimental results. This way the validation of the nozzle geometry was carried out with confidence.

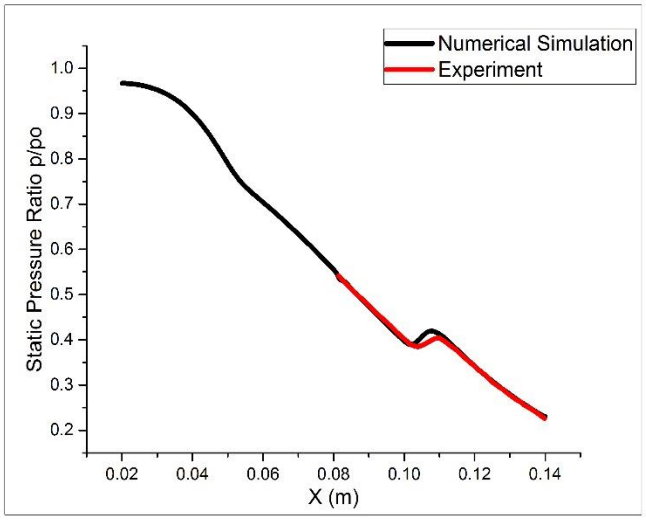

Fig. 4: Comparison of pressure distribution along the centerlinefor a smooth nozzle.

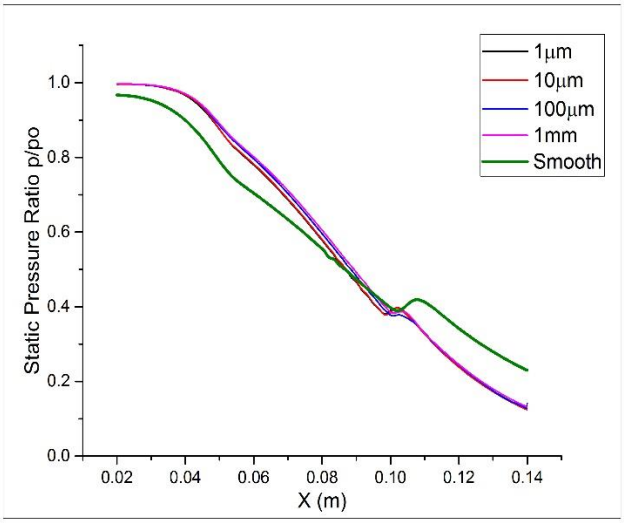

Fig. 5: Pressure distribution along the nozzle length for different equivalent sand grain roughness K_s.

The graphs in Fig.5, 6 and 7 show the variation of different parameters with change in equivalent sand grain roughness. Fig. 5 shows the pressure distribution along the nozzle centerline for different Ks values. It is observed from the graphs that the pressure bump that can be seen for the case with smooth walls is attenuated for the case with different roughness. Initially, up till the throat of the nozzle, the pressures for the cases with roughness is higher when compared with the case without roughness. As the roughness increases, the pressure at the throat for rough nozzles also increase. But after the throat when the condensation shock appears, the shock strength is much lower than that of the smooth nozzle. This is evident from the values provided in Table 1 which shows there is a reduction in the static pressure ratio p/po and therefore in the static pressure values. The percentage reduction in the peak value of the condensation shock produced by nozzles of different roughness values when compared with the nozzle having a smooth surface is also provided in the table. It is seen that there is approximately a 5% reduction in the shock strength for nozzles with Ks = 1μm and 10μm, whereas about 10 % and 8 % reduction for the nozzle with Ks = 100μm and 1mm.

Table 1: Percentage reduction in the pressure peak due to condensation shock w.r.t. $K_s = 0$ for different K_s values.

K_s	**0**	**1μm**	**10μm**	**100μm**	**1mm**
X (m)	0.108	0.102	0.102	0.103	0.104
$(p/p_o)_{max}$	0.419	0.397	0.396	0.377	0.386
Static Pressure (Pa)	29632	28135.1	28110.2	26689.4	27302.1
Percentage Reduction w.r.t. $K_s = 0$	0	5.05 %	5.13 %	9.93 %	7.86 %

Fig. 6 shows the average radius of droplets being formed at the center line with different Ks. The liquid mass starts to get generated at around 0.075m from the inlet. It is at this point that the droplets nucleate in the flow. It is evident from the graph that as the roughness height increases the point of incipience of the droplets shifts further downstream. As the roughness decreases the average radius of the droplets increase. Therefore, the average radius of the newly formed droplets is higher for a smoother surface. The values of the average droplet radius at 0.105m axial distance is tabulated and the percentage reduction in the average droplet radius on increasing the surface roughness is given in Table 2. The average radius of the droplets decreases by 3.16 % if the surface roughness increases from 1μm t o10μm. It reduces by 8.61 %

when roughness increases from 10µm to 100µm. It further drops by 1.31 % if the roughness increases from 100µm to 1mm.

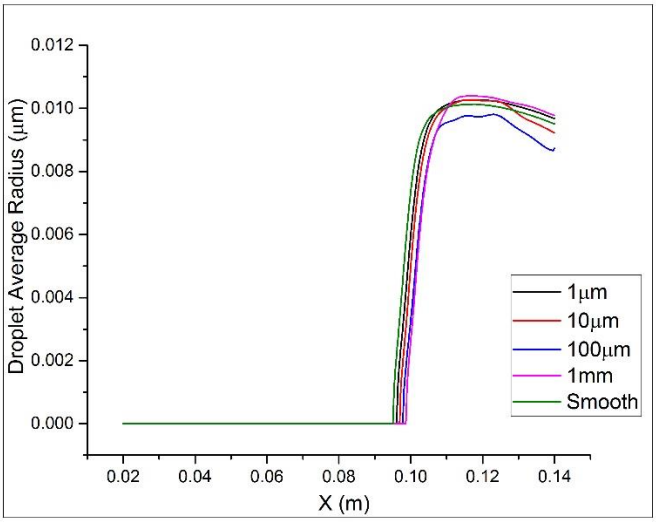

Fig. 6: Droplet average radius variation with K_s.

Table 2: Percentage reduction in droplet average radius.

K_s	**Droplet Average Radius (microns) at X = 0.105 m**	**Percentage Reduction**
1µm	0.00947	0
10µm	0.00917	3.16 %
100µm	0.00838	8.61 %
1mm	0.00827	1.31 %

Fig. 7 shows the variation in the nucleation rate of the droplets with the variation in the surface roughness height. The peak for all the graphs are approximately equal, but, as the surface roughness is increased, the nucleation rate comes down at the throat. Also, for a smoother nozzle wall, the nucleation in the flows begins early and reaches a maximum earlier. The value of nucleation rate is provided in Table 3 at an axial distance of 0.09m. The nucleation rate decreases by 4.24 % as the roughness increases from 1µm to 10µm, 2.50 % when it increases from 10µm to 100µm and then by 4.77 % when it increases from 100µm to 1mm.

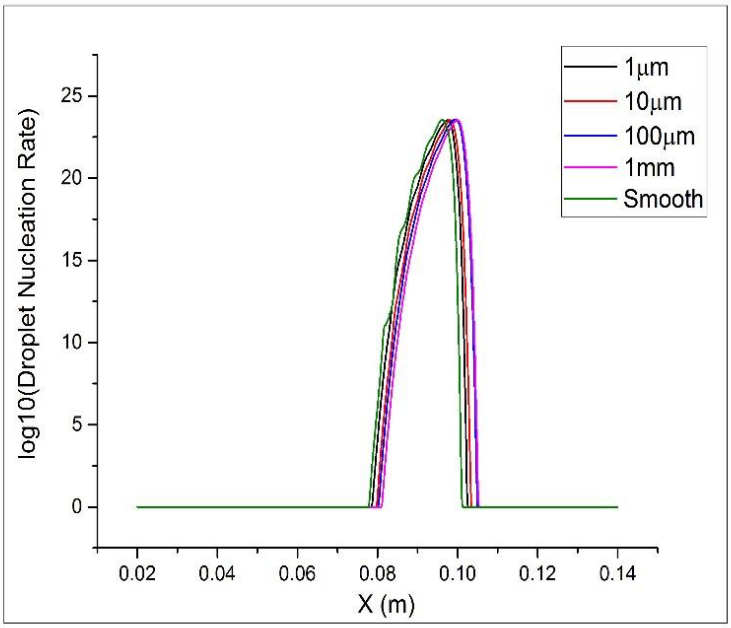

Fig. 7: Nucleation rate variation with K_s.

Table 3: Percentage reduction in nucleation rate.

Ks	Log10(Droplet Nucleation Rate) at X = 0.09 m	Percentage Reduction
1µm	19.5153	0
10µm	18.6863	4.24 %
100µm	18.2175	2.50 %
1mm	17.3473	4.77 %

Surface roughness can alter the nozzle throat area so as to affect the passage flow rate. A variation in the mass flow rate at the inlet and also at the outlet was observed. Table 4 depicts the values of mass flow rates at inlet and outlet for different surface roughness values. As can be seen from the table, as the surface roughness height is increased, the mass flow rate decreases. With the increase in the height of the surface roughness, the effective area for the flow decreases and with the decrease of the flow area, the mass flow rate decreases. With a decrease in mass flow rate of steam the power produced by the turbine also decreases.

Table 4: Mass flow rate for different K_s values.

K_s	**m_{in} (kg.s^{-1})**	**m_{out} (kg.s^{-1})**
0	0.00896162	-0.00896440
1µm	0.00867802	-0.00867673
10µm	0.00854309	-0.00853175
100µm	0.00819936	-0.00834347
1mm	0.00810734	-0.00795875

Gibbs free energy of condensation on a surface is less than that for nucleation. As the surface roughness is increased, it is easier for the steam to condense and therefore for the reduced Gibbs energy the nucleation rate is decreased [17]. For a given wetness fraction if the droplet diameters are smaller, then the number of droplets formed are more and condensation of vapour can happen on a greater surface area. Therefore, smaller droplets cause a reduction in the nucleation rate. As the nucleation rate is reduced and the average radius of the droplets are also lesser, less latent heat is given back to the vapour flow and therefore the condensation shock strength is reduced.

Therefore, it is seen that on increasing the value of the height of surface roughness, the nucleation rate, average droplet radius, and the mass flow rate is decreased. But the increase in the surface roughness cannot be indefinite as surface roughness gives rise to different kinds of losses [9] and also reduces the power produced due to a reduction in the mass flow rate. Hence, a suitable common ground has to be found by optimizing the different parameters so that acceptable amount of power is produced and a surface roughness appropriate to reduce the nucleation rate and wetness at the end of expansion with a reduction in condensation shock strength is maintained.

5. Conclusion

The following conclusions can be drawn from the present study –

1. There is an attenuation of condensation shock strength due to the roughness of the nozzle walls.
2. As the height of the surface roughness increases the average radius of the droplets just after the throat decreases.
3. As the height of surface roughness increases the point of droplet formation shifts downstream.
4. The nucleation rate at the throat of the nozzle decreases as the height of surface roughness increases.
5. The nucleation of the droplets occurs early for a nozzle wall with a smoother surface.
6. The mass flow rate of steam in the nozzle decreases with an increase in the surface roughness.

References

[1] A. G. Gerber and M. J. Kermani, "A pressure based Eulerian–Eulerian multi-phase model for non-equilibrium condensation in transonic steam flow," *International Journal of Heat and Mass Transfer*, vol. 47, no. 10-11, pp. 2217-2231, 2003.

[2] F. Bakhtar, E. Ebrahimi and R. A. Webb, "On the performance of a cascade of turbine rotor tip section blading in nucleating steam Part 1: surface pressure distributions," *Proceedings of the Institution of Mechanical Engineers, Part C: Journal of Mechanical Engineering Science*, vol. 209, p. 115, 1995.

[3] F. Bakhtar, J. B. Young, A. J. White, and D. A. Simpson, "Classical Nucleation Theory and Its Application to Condensing Steam Flow Calculations," *Archive Proceedings of the Institution of Mechanical Engineers Part C-Journal of Mechanical Engineering Science*, vol. 219, 2004.

[4] A. J. White, J .B. Young, and P. T. Walters, "Experimental Validation of Condensing Flow Theory for a Stationary Cascade of Steam Turbine Blades," *Phil Trans. R. Soc. Lond*., vol. 354, pp. 59-88, 1996.

[5] J. B. Young, "Two-Dimensional, Nonequilibrium, Wet-Steam Calculations for Nozzles and Turbine Cascades," *Journal of Turbomachinery, Transactions of the ASME*, vol. 114, pp. 569-579, 1992.

[6] P. P. Wegener, "Condensation Phenomena in Nozzles," *Progress Astron. Aero.*, vol. 15, p. 701, 1964.

[7] G. Gyarmathy, "Kondensationsstoss-Diagramme fur Wasserdampfstromungen," *Forsch. Ing. Wes.*, vol. 29, pp. 105-114, 1963.

[8] G. Gyarmathy, H. Meyer, *Spontane Kondensation (VDI Forsch.-Heft 508).* Dusseldorf, VDI Verlag, 1965.

[9] H. B. Esfe, M. J. Kermani, M.S. Avval, "Effects of surface roughness on deviation angle and performance losses in wet steam turbines," *Applied Thermal Engineering*, vol. 90, pp. 158-173, 2015.

[10] K. Bammert, H. Sandstede, "Measurements of the boundary layer development along a turbine blade with rough surfaces*," J. Eng. Gas. Turbines Power*, vol. 102, pp. 978-983, 1980.

[11] R. J. Kind, P. J. Serjak, M. W. P. Abbott, "Measurements and prediction of the effects of surface roughness and deviation in a turbine cascade," *J. Turbomach.*, vol. 120, pp. 20-27, 1998.

[12] Y. I. Yun, I. Y. Park, S. J. Song, "Performance degradation due to blade surface roughness in a single-stage axial turbine," *J. Turbomach*., vol. 127, pp. 137-143, 2005.

[13] Q. Zhang, M. Goodro, P. M. Ligrani, et al., "Influence of surface roughness on the aerodynamic losses of a turbine vane," *J. Fluids Eng*., vol. 128, pp. 568-578, 2006.

[14] C. A. Moses and G. D. Stein, “On the Growth of Steam Droplets formed in a Laval Nozzle using both Static Pressure and Light Scattering Measurements,” *Journal of Fluids Engineering*, vol. 100, pp. 311-322, 1978.
[15] W. Wróblewski, S. Dykas, A. Gepert, “Steam condensing flow modeling in turbine channels,” *Int. Journal of Multiphase Flow*, vol. 35, pp. 498-506, 2009.
[16] F. Bakhtar, K. Zidi, “Nucleation phenomena in flowing high-pressure steam: experimental results,”
[17] A. A. Nicol and J. O. Medwell, “Effects of Surface Roughness on Condensing Steam,” *The Canadian Journal of Chemical Engineering*, 1996.
[18] T. Cebeci, P. Bradshaw, *Momentum Transfer in Boundary Layers*. Hemisphere Publishing Corporation, New York, 1977.